Mathematical Medicine and Biology (2006) **23**, 79–99
doi:10.1093/imammb/dql003
Advance Access publication on March 1, 2006

Development of regular cellular spacing in the retina: theoretical models

STEPHEN J. EGLEN†
Department for Applied Mathematics and Theoretical Physics, University of Cambridge, Wilberforce Road, Cambridge CB3 0WA, UK

[Received on 18 May 2005; accepted on 29 September 2005]

During development of the nervous system, neurons should be appropriately positioned to enable them to make the right functional contacts. Neurons do not immediately migrate to their correct location, but instead regular arrangements gradually emerge from randomly arranged cell populations. This phenomenon has been studied often in the retina, due to its relatively simple layered organisation. In this review, I highlight the principal mechanisms that are thought to be involved, and how mathematical modelling has helped to further our understanding of the role of these processes upon mosaic formation. Three developmental mechanisms are studied in detail, namely, lateral migration, cell fate and cell death. As a case study, I then consider which mechanisms might be involved in the formation of retinal ganglion cell mosaics.

1. Nature and formation of retinal mosaics

The retina is assembled as a stack of several cell layers, with the photoreceptors in the outermost layer and the retinal ganglion cells (RGCs) in the innermost layer (Fig. 1). Photoreceptors convert light into electrical activity which is then modulated by the interacting vertical and horizontal neural pathways within the retina. Once the activity reaches the RGCs, it is converted into spike trains which are sent along the optic nerve and into subcortical and cortical areas in the brain for higher processing. For a comprehensive review of retinal architecture and processing, see Rodieck (1998). The organisation of the retina obeys certain principles which make it relatively easy to study compared to other parts of the nervous system, such as neocortex. For example, there are five major classes of retinal neuron, each with clearly defined morphologies. Each class of retinal neuron tends to be found in one vertical layer, making cell identification easier. Following the terminology of Cook (1998), each class divides into subclasses of neurons which in turn can be classified into individual types of retinal neuron.

At the level of individual cell types, we typically find the spatial organisation of cells within a type to be highly non-random (Fig. 2a). This regular organisation of cell bodies is referred to as a 'retinal mosaic' due to the way that the cell body (and its dendrites) tiles the retina. This regular organisation makes sense from the point of view of processing the visual world: receptors are needed uniformly across the retina to ensure that the visual world is regularly sampled and that there are no 'holes' in visual space. In this review, I will discuss recent mathematical models that have helped us investigate how these retinal mosaics form during development. I will first review the neurobiological background about the mechanisms that are thought to be involved, and review several types of model, before focusing on a case study comparing how different models may account for the positioning of RGCs.

As well as gaining an insight into the formation of neural patterning in retina, the hope is that we may also learn something about the principles underlying development of the nervous system in general.

†Email: S.J.Eglen@damtp.cam.ac.uk

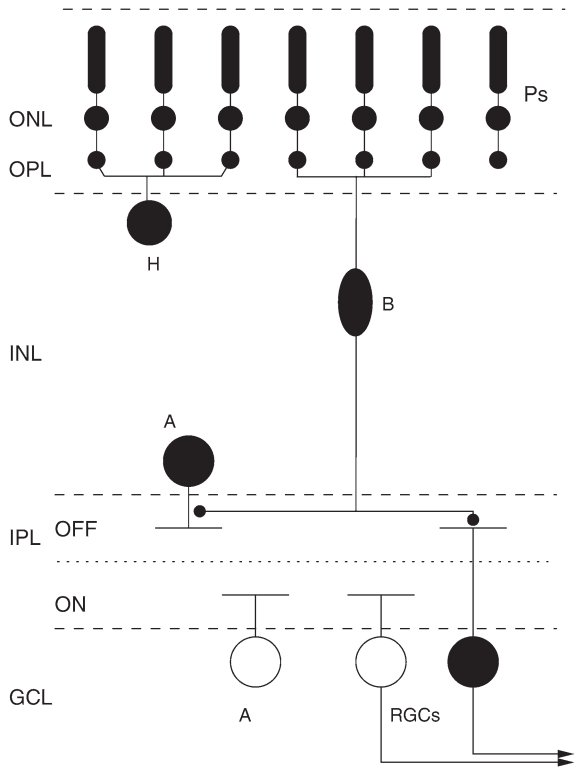

FIG. 1. Schematic showing the layered architecture of a typical adult vertebrate retina and cellular positioning. Light enters the eye and is converted into electrical activity by photoreceptors (Ps). A lateral pathway of horizontal cells (H) mediates lateral interactions, as signals propagate vertically through bipolar cells (B) to reach the RGCs. Amacrine cells (A) either side of the inner plexiform layer (IPL) provide a second stage of lateral processing. RGCs are the only cells that send axons (arrowheads) out of the retina to form the optic nerve. Cells that depolarise in response to light are drawn as open symbols, whereas those cells that hyperpolarise to light are filled. The names of layers are given to the left: ONL, outer nuclear layer; OPL, outer plexiform layer; INL, inner nuclear layer; GCL, ganglion cell layer. The IPL can be divided into on- and off-sublayers to account for the different responses of on- and off-centre RGCs (see Section 7).

Many parts of the nervous system may use a modular architecture of connections to simplify the task of wiring up functional circuits. The retina is a good system to investigate organisational principles due to the limited number of cell types, its clear division into vertical layers and the availability of suitable neurochemical markers for staining cells. Observing regular distributions of neurons in other systems is harder due to the much wider diversity of cell types and the difficulty in classifying them (Cook & Chalupa, 2000).

2. Biological mechanisms involved in development of neuronal mosaics

Postmitotic cells in the developing retina are multipotent: they have the ability to develop into any of a number of different cell types, depending on fate determination events. These cell fate events are influenced by a combination of factors intrinsic to the cell and extrinsic signalling factors in the surrounding tissue (Livesey & Cepko, 2001). Once cells stop dividing in the ventricular zone (located near the region that eventually becomes the photoreceptor layer), they migrate radially down to their destination

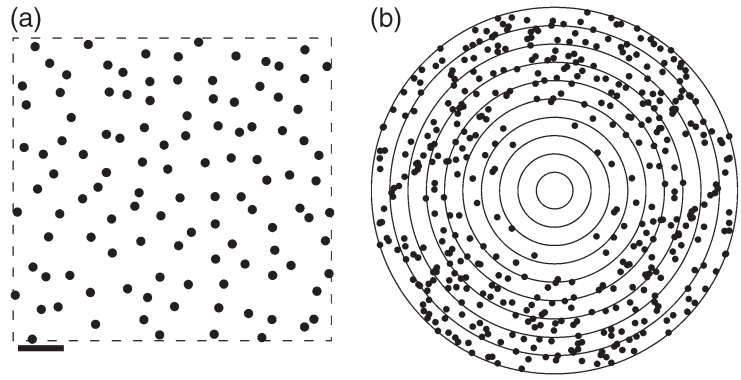

FIG. 2. Spatial distribution of cholinergic amacrine cells in the inner nuclear layer from a rat 12 days old (P12). (a) Location of all cell bodies. Dotted line indicates extent of the sampling window used to record cell positions. Scale bar: 50 μm. Cell bodies are drawn to scale (10 μm diameter). The RI of this field is 5.1. (b) Autocorrelation plot of the field shown in (a). Each small circle indicates the position of one cell relative to another cell. Annuli are drawn 5 μm apart. No two cells tend to be less than 15–20 μm apart. (Cells in (b) are not drawn to scale for clarity.) Data kindly provided by Dr Lucia Galli-Resta.

layer, and can also move tangentially within a layer. Upon arrival in the correct destination layer, cells begin making synaptic connections to their targets. Throughout these phases of cell fate, migration and differentiation, there is ongoing cell death in all classes of retinal neuron, helping to sculpt out the adult distribution of cells. In this section, I briefly review these biological mechanisms and summarise how mosaic regularity is typically quantified.

2.1 *Cell fate mechanisms*

The different classes of retinal cell are typically born in an ordered developmental sequence: RGCs, cone photoreceptors, amacrine, horizontal cells, bipolar cells and rod photoreceptors (Robinson, 1991). However, at any one time in development, the windows of birth for each cell class overlap and so postmitotic neurons are not constrained solely by their birth date as to their eventual identity. Instead, extrinsic signalling factors, possibly released by neighbouring cells, influence the fate of individual cells to acquire a particular identity (Livesey & Cepko, 2001). For example, RGCs secrete factors that inhibit neighbouring cells from also becoming RGCs (Waid & McLoon, 1998).

2.2 *Radial and tangential migration*

Early work on the analysis of cell migration from the ventricular zone suggested that cells moved radially down into their destination layer, thus forming columns of cells that were clonally related to each other (Turner & Cepko, 1987). In this view, the positioning of retinal neurons is constrained by the position of the postmitotic cells in the ventricular zone. However, two recent lines of evidence counter this suggestion. First, by using a transgenic mouse model where 50% of all clones were labelled, it could be observed that certain classes of retinal neuron moved tangentially away from their clonal column of origin. Furthermore, the cells that underwent lateral migration belonged to the classes of retinal neuron that are most regular. Cells typically moved 20–100 μm laterally, and for those cell types that moved, normally all cells within a type moved laterally (Reese *et al.*, 1995, 1999). Second, observation of cholinergic amacrine cells at different times during their migration showed that migrating cells were often side-by-side, and yet once they arrived in their destination layer, they were more regularly

spaced apart (Galli-Resta *et al.*, 1997). Many retinal neurons therefore move both radially away from the ventricular zone and laterally within their destination layer.

2.3 *Cell death*

Throughout the nervous system, many more neurons are born during development than those that ultimately survive into adulthood. In the case of the RGCs, estimates from a range of species indicate 50–90% of RGCs die during development (Finlay & Pallas, 1989). Although this cell death has previously been linked to the elimination of RGCs that make inappropriate connections in their target areas (O'Leary *et al.*, 1986), cell death could also be useful in sculpting the retinal mosaic distributions (Cook & Chalupa, 2000). In developing cat retina, the postnatal increase of mosaic regularity of alpha RGCs was correlated with a 20% loss in the density of RGCs. This suggested that cell death might be responsible for the increase in mosaic regularity, perhaps by eliminating close pairs of neighbouring neurons (Jeyarasasingam *et al.*, 1998). The high levels (up to 90%) of cell death inferred in mouse retina has been suggested to be responsible for creating the mildly regular arrangement of dopaminergic amacrine cells (Raven *et al.*, 2003). Finally, cell death induced by extracellular adenosine triphosphate kills cholinergic amacrine cells that are too close to each other, therefore changing cellular spacing (Resta *et al.*, 2005). However, cell death does not always have an instructive role, since e.g. mosaic regularity was constant during the period 4–12 days after birth, when around 20% of cholinergic amacrines typically die (Galli-Resta & Novelli, 2000).

2.4 *Evaluating mosaic regularity*

The regularity index (RI) has long been used as the benchmark index for evaluating the regularity of a group of retinal neurons (Wässle & Riemann, 1978). For each neuron, we measure the distance to its nearest neighbouring cell of the same type; RI is then defined as the mean/s.d. of these nearest neighbour distances. The higher the RI, the more regular the pattern; retinal mosaics typically have indexes in the range 3–9, and, typically, values above 2 indicate non-randomness (Wässle & Riemann, 1978; Cook, 1996). Many other measures have been proposed, including those based on quantifying the size of the exclusion zone in autocorrelograms (Rodieck, 1991) and various Voronoi-based measures, such as Voronoi domain area (Galli-Resta *et al.*, 1999).

3. The exclusion zone approach

The cell bodies of most types of retinal neurons space themselves out so that they are not too close to other neurons of the same type (Fig. 2a). By performing an autocorrelation on the position of the cell bodies, we typically find that there is a central hole in the autocorrelation which defines the empty space around each cell. For example, for the field shown in Fig. 2a, the autocorrelation plot in Fig. 2b shows that typically no two cholinergic cells come closer than 15–20 μm of one another. The empty space around a cell body is commonly termed an 'exclusion zone'. Furthermore, cross-correlation analysis of two different cell types (measuring the relevant displacement between pairs of cells of opposite types) typically shows no such exclusion zone, and hence a lack of spatial interaction between cells of different types (Rockhill *et al.*, 2000). Hence, interactions are thought to be mostly homotypic (i.e. interactions are limited to between neurons of the same type), although some exceptions have been reported (Kouyama & Marshak, 1997; Ahnelt *et al.*, 2000).

Several older models have investigated the effects of such an exclusion zone upon the spacing of retinal neurons otherwise positioned randomly in neural tissue (Diggle & Gratton, 1984; Shapiro *et al.*,

1985; Scheibe *et al.*, 1995). However, in recent years, work by Galli-Resta *et al.* have tested exclusion zone models on many types of retinal neurons. Their model is called the '$d_{\min}$ model', named after the $d_{\min}$ parameter which specifies the diameter of the exclusion zone for each cell.

3.1 *Methods*

The $d_{\min}$ model uses a sequential algorithm for cell positioning. Starting with an empty area A, trial cells are added serially into the array. A trial cell is positioned at random somewhere within A, and it is given a $d_{\min}$ value drawn from a Gaussian distribution. If the nearest neighbouring cell is further away than $d_{\min}$, the trial cell is accepted into the array, otherwise the trial cell is rejected. This process terminates either when the desired number of cells have been added into A or if no more cells can be added due to packing limits. (The serial nature of this algorithm means that the typical maximal packing density is around 0.55 compared to theoretical limits around 0.91 for hexagonally arranged cell bodies; Tanemura, 1979; Diggle, 2002.)

Hence, to model a retinal distribution using the $d_{\min}$ model, the main parameters required are the mean and s.d. of the $d_{\min}$ Gaussian distribution; the number of cells and the size of A normally matches the experimental data being modelled. To date, finding suitable exclusion zone parameters has usually relied on ad hoc searching over parameter space, but we have recently started using maximum likelihood estimation techniques for parameter estimation (Diggle *et al.*, 2006).

3.2 *Results*

This model has successfully replicated the spatial distribution of many types of retinal neuron, including cholinergic amacrine cells, photoreceptors, RGCs and dopaminergic amacrine cells (Galli-Resta *et al.*, 1997, 1999; Cellerino *et al.*, 2000; Raven *et al.*, 2003). Figure 3 shows an example of the application of the $d_{\min}$ model to two different types of mosaics. In both cases, the $d_{\min}$ model can accurately replicate the spatial distribution of these cell types.

In many vertebrate retinas, the density of a given type of retinal cell tends to be much higher in central retina than in the periphery. By fitting the model to a range of fields acquired at different retinal eccentricities (and thus of different densities), Galli-Resta *et al.* were able to test whether $d_{\min}$ would vary or not across the retina. Interestingly, they found differing results depending on the data sets being examined. In the photoreceptors of ground squirrel, the same $d_{\min}$ distribution could replicate the mosaics observed at different densities; as a result, the RI increased with increasing cell density (Galli-Resta *et al.*, 1999).

By contrast, reduced nicotinamide adenine dinucleotide phosphate (NADPH)-diaphorase RGCs in chick retina have a constant RI (6.3 ± 0.8) across different cell densities, and thus one $d_{\min}$ distribution could not account for these mosaics. In this case, the authors suggested that the cells might be created by the 'little bang' hypothesis proposed by Rodieck & Marshak (1992). This hypothesis suggests that neurons are initially closely packed across the retina at a time when the retina is still quite small. As the retina then stretches non-uniformly during development, the cells then space out to different degrees, but with the same regularity.

3.3 *Evaluation*

The exclusion zone models show us that local interactions, based on inhibiting neighbours from coming too close to each other, are sufficient to replicate the patterns observed in wide types of retinal neurons. However, as acknowledged by Galli-Resta *et al.* (1997), the model suggests that an exclusion zone

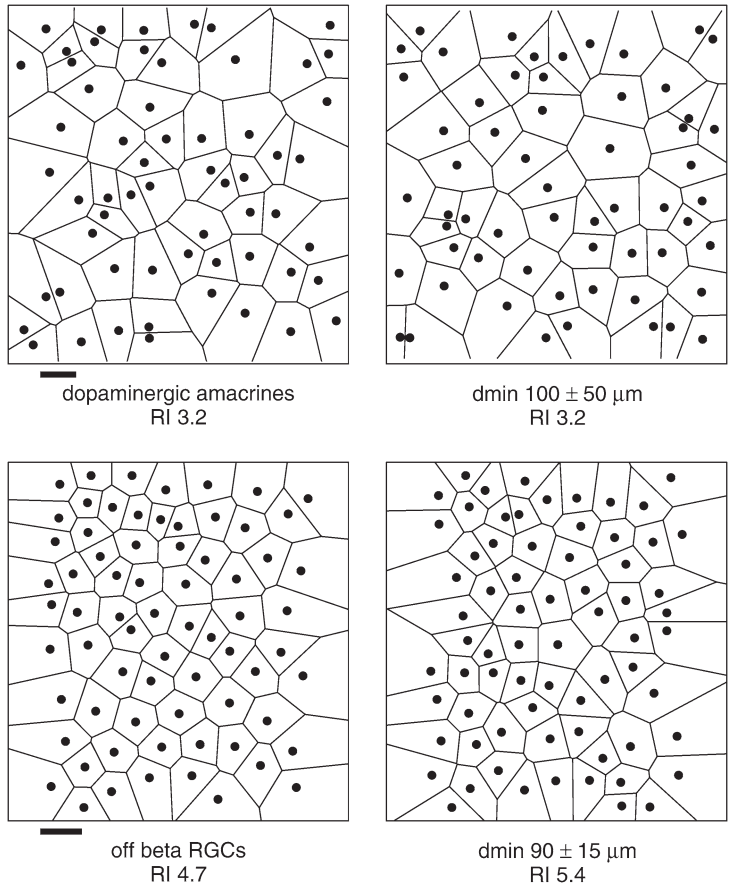

FIG. 3. Examples of the application of the $d_{\min}$ model to two different datasets. Top: dopaminergic amacrine cells from the mouse retina can be replicated using $d_{\min} = 100 \pm 50$ μm (mean ± s.d.). Likewise, cat off beta RGCs (bottom) can be modelled with $d_{\min} = 90 \pm 15$ μm. Each cell is drawn with its surrounding Voronoi polygon. Beneath each plot is the RI of the mosaic. Scale bars: 100 μm. Experimental data taken from Wässle *et al.* (1981a) and Raven *et al.* (2003).

mechanism 'can generate the mosaics, not that it actually does'. Evidence is therefore needed as to how the exclusion zone might be enforced in a biological system. One possibility is that trial cells which are too close to existing positioned cells will die; however, the number of trial cells generated during a simulation can soon far exceed the estimates of the levels of cell death in the developing retina.

Another possibility might be that each cell releases a diffusible substance that other cells respond to. Recent modelling of goldfish retinal neurons suggests that a diffusible substance might control cell fate decisions to regulate neuronal spacing (Cameron & Carney, 2004; Tyler *et al.*, 2005). In the goldfish retina, new neurons are continually added to the circumferential germinal zone (CGZ), at the outer edge of the retina, throughout life. By assuming that each differentiated neuron of a given type releases a diffusible substance that decays exponentially with distance, each newborn neuron within the CGZ was inhibited from acquiring a certain fate unless the local level of diffusible substance was less than a certain threshold. By appropriate setting of the decay constants for each diffusible substance, the model was able to replicate the spatial distribution of two types of neuron.

This modelling work therefore suggests that an exclusion zone could be sculpted by a diffusible substance preventing newborn neurons in close proximity from adopting the same fate. Such a mechanism may be appropriate for fish retina, but is unlikely to be universal. For example, in rat, analysis of close pairs of neurons (where intuitively one would expect higher levels of the proposed diffusible substance if each cell independently releases the substance) suggests that pairs of cells do not have larger exclusion zones than single cells, and so diffusible signals are unlikely (Galli-Resta, 2000).

A technical issue with the $d_{\min}$ model is that once a cell is positioned in the array A, it does not then move as later cells are added into the array—this is highly unlikely to happen biologically; instead, cells are likely to be much more mobile, especially when dendrites are immature. However, this does not apply to all exclusion zone models—some can be implemented in a 'birth and death' manner, whereby all cells are initially placed at random, and then each cell dies and is reborn elsewhere in the field many times until convergence is achieved (Ripley, 1977; Diggle *et al.*, 2006; Eglen *et al.*, 2005). Alternative mechanistic explanations for the exclusion zone are considered in subsequent sections.

4. Lateral movement model

In one of the earliest papers describing the properties of retinal mosaics, one hypothesis for their formation was given: each cell has a repulsive force which helps transform a random arrangement into a regular pattern of cell bodies (Wässle & Riemann, 1978). This suggestion was implemented in a model of lateral cell migration, described here (Eglen *et al.*, 2000). The lateral movement model is based on an earlier model of neurite outgrowth, investigating the role of intracellular calcium levels ($[Ca^{2+}]_i$) upon neurite outgrowth (van Ooyen & van Pelt, 1994). Intracellular calcium levels are regulated by many processes, but for this model we assume that only neuronal activity modulates $[Ca^{2+}]_i$. In this model, low $[Ca^{2+}]_i$levels drove neurite extension, and high $[Ca^{2+}]_i$levels caused their retraction. For cells positioned randomly within a surface A, the size of each neuron's neurites was inversely proportional to the local density (van Ooyen & van Pelt, 1994). This was the starting point for our model, whereby we allowed cells to both extend neurites and move laterally.

4.1 *Methods*

The model contains n cells positioned on a surface A. Each cell i is represented by three variables: ($\mathbf{C}_i$, R_i, X_i). $\mathbf{C}_i$(bold denotes a 2D vector) is the location of the cell body, and R_i is the radius of its (circular) dendritic field. X_i is the mean membrane potential, which reflects its intracellular calcium concentration. Each cell is initially positioned at random within A and R_i and X_i are both zero. The following differential equations then update each variable:

1. X_i is regulated by a weighted function of inputs from neighbouring cells:

$$\frac{\mathrm{d}X_i}{\mathrm{d}t} = -\frac{X_i}{\tau} + (1 - X_i)\sum_{j=1}^{N} W_{ij} F(X_j), \tag{4.1}$$

$$\text{where } F(X_j) = \frac{1}{1 + \exp[(\theta - X_j)/\alpha]}, \quad W_{ij} = cA_{ij}.$$

$F(X_j)$ is the mean firing rate of cell j. A_{ij} is the area of overlap between the dendrites of cell i and j. The input from cell j to cell i, W_{ij}, is cA_{ij}, where c is a constant representing synaptic strength.

2. The rate of dendritic outgrowth depends on the cell's mean firing rate:

$$\frac{\mathrm{d}R_i}{\mathrm{d}t} = \rho G(F(X_i)), \tag{4.2}$$

$$\text{where } G(x) = 1 - \frac{2}{1+\exp[(\epsilon - x)/\beta]}.$$

$G(x)$ is typically a sigmoidal function $G(x)$; when the cell's firing rate is below the threshold ϵ, $G(F(X_i))$ is positive, causing outgrowth. Conversely, when it is above threshold, $G(F(X_i))$ is negative, causing retraction of the dendritic field.

3. Cell bodies repel each other at a rate proportional to their dendritic overlap:

$$\frac{\mathrm{d}\mathbf{C}_i}{\mathrm{d}t} = \eta \sum_{j=1}^{N} u(\mathbf{C}_i - \mathbf{C}_j) W_{ij}. \tag{4.3}$$

$u(\mathbf{V})$ is the vector $\mathbf{V}$ normalised to unit length, except $u(\mathbf{0}) = \mathbf{0}$. Elements of $\mathbf{C}_i$ are bounded to keep each cell body within the surface A. Full parameters are given in Eglen *et al.* (2000).

4.2 *Results*

The typical developmental sequence observed in the lateral movement model is shown in Fig. 4. In the first stage of development, since neurites start out small, there is little overlap between neighbours and thus low levels of $[Ca^{2+}]_i$. This causes dendrites to extend effectively to seek out inputs from neighbouring cells. At this stage, since dendrites barely overlap, there is no repulsion between cells. In the second stage, once dendrites have increased in size, they then begin to overlap and repel each over, causing some mild increase in regularity (Fig. 4b). This process continues until eventually cells stabilise into a regular arrangement (Fig. 4c) with most cells having similar-sized dendritic fields. In this model, all cells move, and the amount of movement is relatively small, within the bounds of that suggested experimentally (Reese *et al.*, 1999).

As a side note, Fig. 4 highlights one key problem faced in this type of modelling: handling boundary effects. Many cells in this simulation have been pushed to the edges of the surface A, and would continue to move outside the region unless explicitly prevented from doing so. Cells at the border therefore have larger dendritic fields as an artifact of the boundary conditions, since they receive input from fewer cells. Toroidal boundary conditions could be introduced to prevent this problem, although, typically, analysis of real and simulated mosaics uses various methods to detect, and account for, cells that lie at the boundary of the sample area (Rodieck, 1991; Raven *et al.*, 2003).

Given the basic model, manipulations can be performed to test various situations. For example, the model copes with a gradual change in the number of cells within the sample; adding more cells to a growing network causes a reduction in the nearest neighbour distances while maintaining a high regularity. Conversely, if some cells die (e.g. simulating a local lesion of tissue), neighbouring cells expand to occupy the empty area, in line with experimental findings (Perry & Linden, 1982).

One problem with the default model is that the mosaics are too regular—with typical RIs of 10–14, they are more regular than those observed in retina. The main reasons for this are the assumption of circular dendritic fields, and the ability to determine exactly the area of overlap A_{ij} between neighbouring neurons. As the area of overlap, A_{ij} is approximated to lower levels of accuracy, the RI at maturity in the model drops to much more realistic values (see Table 1 of Eglen *et al.*, 2000). Also, if A_{ij} instead

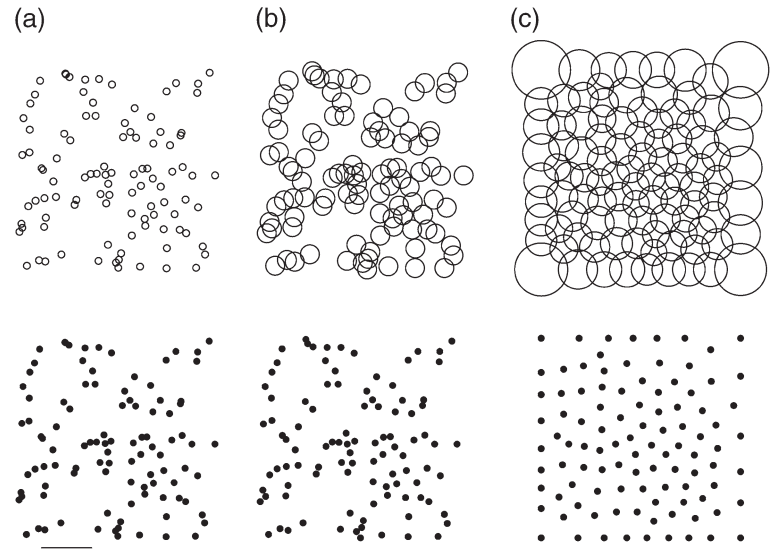

FIG. 4. Development of regularity in the dendritic interaction model. In the upper plot, each circle represents a neuron with radius equal to dendritic extent; the lower plot shows just the cell body of each neuron. The same network is shown at three stages of development. (a) Early in development, dendrites have just started growing; since there is no significant overlap, there is not yet lateral movement and so the mosaic is close to random (RI = 2.4). (b) A little while later, dendrites have extended enough to overlap and cause some small movement and a slight increase in mosaic regularity (RI = 3.3). (c) Towards the end of the simulation, dendrite sizes are uniform and the mosaic is highly regular (RI = 9.0). The rectangular bounds of the area can clearly be seen; cells can be pushed towards, but not beyond, this boundary. Scale bar: 100 μm.

measures the relative, rather than absolute, degree of overlap between neighbouring neurons, we find that dendritic area varies inversely with the density of neurons. The model therefore replicates a fundamental feature of retinal dendrites, namely, that they have constant coverage factor (the product of density and dendritic area) of the retina despite the large central–peripheral density gradient (Sterling, 1983). Finally, within the model, if dendritic fields do not change size, we find that cell movement is no longer universal, and that regularity is proportional to the dendritic field size and the number of cells. In this situation, the lateral movement model is functionally similar to the $d_{\min}$ model, by equating $d_{\min}$ with $2R_i$. Over a wide range of values of $d_{\min}$, the two models produce mosaics of similar RIs (Eglen *et al.*, 2003).

4.3 *Evaluation*

The lateral movement model hypothesises that the observed tangential movements of retinal neurons can be driven by interactions between neighbouring dendrites. By suitably choosing a way of calculating the overlap between neighbouring dendrites (A_{ij}), the model is able to replicate mosaics with a range of RIs that covers those observed experimentally (and beyond, depending on the accuracy of A_{ij}).

What evidence is there that such lateral movement might be regulated by dendritic interactions? First, horizontal cells have radial processes while migrating around the time of birth, which then change to being horizontally aligned within the outer plexiform layer a few days later. This change in morphology coincides with the estimated time of their tangential dispersion (Reese *et al.*, 1999). Furthermore, dendritic networks are responsible for the maintenance of mosaic assembly. Pharmacological disruption of microtubules within dendrites of cells already organised into regular arrays causes cells to

rearrange from a regular to irregular mosaic (Galli-Resta *et al.*, 2002). Furthermore, after the effects of the pharmacological agents have worn off, the regular spacing of cells gradually returns. This finding led Galli-Resta *et al.* to suggest a micromechanical model of mosaic formation where dendrites form a mechanical network that keeps the cells spaced apart. This suggestion has recently been implemented in a mathematical model that replaced (4.1) and (4.2) with a set of equations representing tensile forces between neighbouring neurons (Ruggiero *et al.*, 2004). Initial results from this model suggest that regular mosaics can form using this approach, although cell bodies seem to converge to a rectangular, rather than hexagonal, lattice due to implementation of the model on a rectangular grid.

5. Modelling of cell fate

Postmitotic cells in the retina commit at some point in development to differentiate into one particular type of neuron. Many cell-intrinsic mechanisms and extracellular signals are important in this process; in this review, I focus on extracellular determinants of cell fate. One common mechanism is that of lateral inhibition, whereby initially undifferentiated cells compete among their neighbours to acquire primary fate; surrounding cells then acquire secondary fate. This process of lateral inhibition has been particularly well studied in Drosophila retina. This retina, unlike vertebrate retinas, is known as a compound eye; the eye is made up of around 800 ommatidia, with each ommatidia composed of eight photoreceptors (R1–R8) organised in a stereotyped manner. The R8 photoreceptor is the first to differentiate; once R8 is specified, surrounding cells are induced to become R1–R7 photoreceptors in a strict temporal sequence. R8 is termed a founder cell as it then induces the fate of surrounding cells. Many molecular markers have now been implicated in controlling the selection of the R8 photoreceptor, including the Delta–Notch signalling system as a form of lateral inhibition (Frankfort & Mardon, 2002). Although the Drosophila compound eye is much more regular than verterbrate retinas, mechanisms observed in Drosophila, such as lateral inhibition, may also operate in vertebrates (Jarman, 2000). In this section, we consider models that have investigated the role of cell fate mechanisms upon formation of retinal mosaics.

5.1 *Modelling of zebrafish photoreceptor mosaic*

The organisation of photoreceptors tends to be slightly different to that of other classes of retinal neuron. The cell bodies of most classes of retinal neuron do not individually cover the entire retina; it is only when we also consider their dendrites that we see the entire surface is covered. By contrast, the cell bodies of photoreceptors tend to be tightly packed together with few gaps between them. This close packing of photoreceptors is presumably to ensure that the visual world is sampled as efficiently as possible. As seen for Drosophila, this means that cell fate mechanisms may well play a role in organising the spatial arrangement of different photoreceptors. Figure 5 shows a schematic of the regular organisation of the cone photoreceptors in zebrafish. There are four types of cone that respond maximally to different parts of the spectrum: red, green, blue and UV sensitive (R, G, B and UV, respectively). Again, these cells differentiate from a population of precursor cells that are presumably able to differentiate into one of several types of cone. (The red and green cones are treated as a special case, in that they always form a double cone (D), arranged in one of four orientations.)

5.2 *Methods*

To investigate how this regular pattern of photoreceptors might develop, Tohya *et al.* (1999) built a stochastic model of cell differentiation. Undifferentiated cells were positioned in a rectangular array

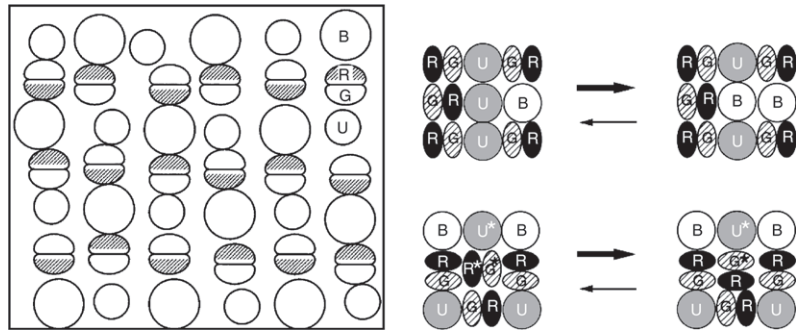

FIG. 5. Zebrafish photoreceptor mosaic and possible mechanisms for changing state. Left: tracing of the outline of cone photoreceptors in zebrafish retina. The red and green cones form a double cone, which can appear in different orientations. These double cones are regularly interspersed with blue and ultraviolet cones. Right: Two examples of possible state changes. In each case, the central cone is the one that potentially changes state. In the top example, changing the U cone to a B increases the stability (i.e. going from left to right is preferred, as shown by relative sizes of arrows). In the bottom example, the double cone is more stable positioned vertically than horizontally. Reprinted from Tohya *et al.* (1999) with permission from Elsevier.

(with toroidal boundary conditions). Each cell was randomly assigned to one class (D, B or UV). Cells were then allowed to transition from one state to another in a continuous time Markov chain. Assuming only one transition happens in time Δt, and that the cell located at position x is currently in state c, the cell may change to state c' with probability

$$p = \frac{2m}{1+\exp[-\Delta E^x/m]}\,\Delta t, \tag{5.1}$$

$$\text{where } \Delta E^x = \sum_{z\in N_x} \lambda_{c',c(z)} - \sum_{z\in N_x} \lambda_{c,c(z)}. \tag{5.2}$$

m is the baseline rate of transitions. The terms $\lambda_{i,j}$ measure the affinity in having a neighbouring pair of cells in state i and j. $c(z)$ is the state of the cell located at position z, neighbouring x (N_x denotes all the neighbours of x). The term ΔE^x therefore measures the change in stability of the change in state of the cell at position x. Figure 5 shows two examples of cells changing state.

5.3 *Results*

To see if this model of cell fate determination could replicate the observed photoreceptor pattern, many possible combinations of the 10 affinities $\lambda_{i,j}$ were evaluated. This task was simplified by setting the four affinities for neighbouring cells of the same type ($\lambda_{i,i}$) to zero, leaving six affinities. For each combination of affinities, the developing pattern was compared with the observed pattern in zebrafish. Out of the 4096 possible combinations tested (assuming four different values for each of the six affinities), only five parameter sets replicated the observed pattern. Their model was therefore able to replicate the natural pattern, but more importantly, as a consequence, predicted the relative affinities needed between neighbouring cells to replicate the cone mosaic. Furthermore, convergence of the model was much quicker if cells gradually differentiated in a row-wise fashion, rather than allowing all cells at once to differentiate. This effectively mimics the 'morphogenetic furrow' observed in developing Drosophila retina, where differentiation proceeds in a moving wave-front across the retina. Such waves of neuronal differentiation has also been suggested to occur in zebrafish retina (Jarman, 2000; Raymond & Barthel, 2004).

However, in the model, the row-wise differentiation is enforced for computational convenience, whereas the wave of differentiation in natural system propagates without external input (Jarman, 2000).

5.4 *Evaluation*

The main contribution of the model of zebrafish cone photoreceptor mosaic is that it has proposed relative affinities of different cell types for one another. Later work by the same group produced an equivalent model, but this time based on cell-sorting mechanisms; pairs of cells swap location as long as it improves the overall affinity of the mosaic (Mochizuki, 2002; Tohya *et al.*, 2003). The model could also account for slight variations between different types of fish mosaic pattern. It is yet to be determined whether the relative affinities between cell types has any relationship to molecular interactions between differentiating cell types. However, out of the two models, cell fate versus cell sorting, cell fate is the more likely biological mechanism. At the earliest ages at which cells can be reliably labelled as a particular type (when the opsin for that type of receptor is first detectable), the photoreceptors are already arranged in a regular pattern. Hence, physical rearrangement of existing photoreceptors is unlikely (Raymond & Barthel, 2004). As an alternative model, Raymond & Barthel (2004) have suggested that there is a cascade of cell fate decisions, starting with the decision for certain cells to become red cones, which in turn instruct neighbouring cells to become blue cones, and so on. This model itself, however, is not complete because it does not address the important question of how red cones are initially organised in a particular spatial pattern.

6. Models of lateral inhibition applied to neurogenesis

The model of zebrafish mosaic organisation modelled stochastic cell fate decisions in a general fashion, based on abstract concepts of affinities rather than using details of known biological processes. One such important process of cell fate is lateral inhibition. An early model of cell fate mediated via lateral inhibition was used to estimate the relative numbers of primary versus secondary fate neurons (Honda *et al.*, 1990; Tanemura *et al.*, 1991).

In this model, lateral inhibition of cell fate was modelled in a simplistic fashion. An array of undifferentiated cell locations was created using an exclusion zone rule (section 3). The Voronoi tessellation of the cell locations was then calculated, and two cells were defined as neighbours if they shared an edge of a Voronoi polygon. From an array of undifferentiated cells, a cell was selected to acquire primary fate; this then induced neighbouring cells to acquire secondary fate. Various different rules were used to decide the order in which cells were selected to acquire primary fate (e.g. selection at random, or a left–right wave of differentiation), and their effect on the ratio of the number of primary:secondary fate cells was calculated. Depending on the choice of rule, different cell ratios were observed (3.3–3.9), in line with the observed ratio of cells destined to become -neuronal versus neuronal (Honda *et al.*, 1990). Such lateral inhibition of cell fate is thought to be mediated by pathways including the Notch–Delta signalling system. This would be particularly appropriate for cell bodies that are in contact with each other, since the ligand Delta is found on the cell surface. This work was followed by a more detailed mathematical model of Delta–Notch signalling (Collier *et al.*, 1996), described next.

6.1 *Methods*

Each cell produces Notch as an increasing function of the level of Delta in its neighbouring cells; Delta production in a cell, however, is a decreasing function of the cell's level of Notch. The levels of Notch

(n_p) and Delta (d_p) in each cell p then evolve according to the following differential equations:

$$\frac{\mathrm{d}n_p}{\mathrm{d}t} = f(\overline{d}_p) - n_p, \tag{6.1}$$

$$\frac{\mathrm{d}d_p}{\mathrm{d}t} = g(n_p) - d_p, \tag{6.2}$$

where $\overline{d}_p$ is the mean level of d in the neighbours of cell p. f and g are suitable increasing and decreasing functions of x:

$$f(x) = \frac{x^k}{a + x^k}, \quad g(x) = \frac{1}{1 + bx^h}, \quad a, b > 0, \;\; k, h \geqslant 1. \tag{6.3}$$

At steady state, the levels of Notch of each cell determine its fate: cells with low levels of Notch acquire primary fate, and cells with high levels of Notch acquire secondary fate. Cells are placed in a regular hexagonal grid, and neighbouring cells defined as those that touch each other.

6.2 *Results*

Mathematical analysis of a two-cell system showed that the homogeneous steady state ($n^* = n_1 = n_2$, $d^* = d_1 = d_2$) is unstable if the feedback is strong enough, i.e. $f'(d^*)g'(n^*) < -1$ (Collier *et al.*, 1996). Under these conditions, although the homogeneous steady state is unstable, the heterogeneous steady state is stable, and hence one cell acquires primary fate and the other cell acquires secondary fate.

Network behaviour in a large, hexagonally arranged, group of cells was investigated using computer simulations. Each cell was initialised with high levels of both Notch and Delta. In the first phase of network development, cells gradually converged onto the unstable homogeneous steady state before diverging to the heterogeneous stable steady state (Fig. 6). At steady state, regular arrangements of primary fate cells could be observed, where each primary fate cell is surrounded by secondary fate cells. Hence, for hexagonally arranged cells, the ratio of primary to secondary fate cells observed was around 3:1.

6.3 *Evaluation*

The generic models of cell fate introduced in this section have shown how the ratio and spatial arrangement of two different types of cell can develop from an undifferentiated population of precursor cells. Honda *et al.* (1990) provided a simple framework for assessing the ability of lateral inhibition to replicate experimental data without providing specific details of the molecular mechanism. By contrast, Collier *et al.* (1996) provided a detailed mathematical and computational investigation of the Notch–Delta system, one of the most well-investigated pathways in neural cell fate determination.

A general limitation of the Collier model is that it produces patterns of short wavelength; subsequent work (that could also be applied to retinal mosaic formation) has considered how juxtacrine signalling can generate patterns of longer wavelengths, and so produce cellular distributions with a wide range of ratios of primary to secondary fate cells (Owen *et al.*, 2000; Webb & Owen, 2004). Delta–Notch signalling has also been modelled in finer detail to test under which conditions different types of pattern can emerge (Meir *et al.*, 2002).

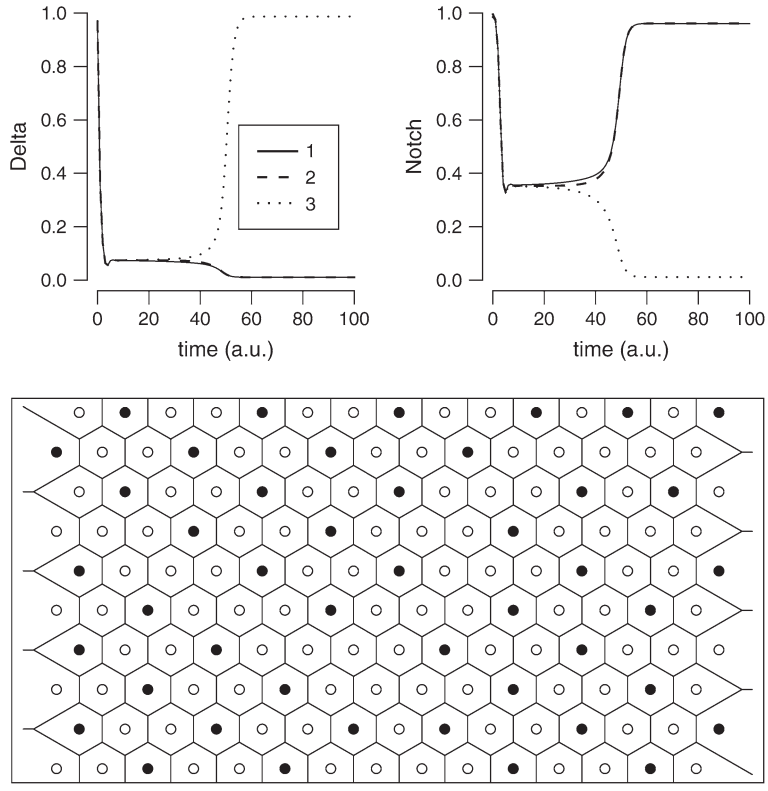

FIG. 6. Emergence of steady state in the Delta–Notch lateral inhibitory model (Collier *et al.*, 1996). Top: Time evolution of Delta and Notch levels for three cells interacting with each other. Initially, the levels of Delta and Notch were set close to 1. After passing close to the unstable homogeneous steady state, the Delta values for cell three (dotted line) start to increase, suppressing Delta in the other two cells. At steady state, cell three acquires primary fate, and cells one and two acquire secondary fate. Bottom: typical outcome for hexagonally arranged cells, where cells interact with just their neighbours. Primary fate cells are coloured black, secondary fate cells are white. A ratio of around 1:3 primary:secondary fate cells is observed. (The ratio is slightly higher than 1:3 due to edge effects.)

7. Case study: beta RGC mosaics

In this section, I consider various mechanisms that have been proposed for the development of RGC mosaics. The RGCs are the only class of neurons that produce action potentials; their axons form the optic nerve which transmits neural activity from the retina to the brain. The RGC class divides into various subclasses, including alpha, beta and gamma. The beta subclass is the biggest in mammals, comprising about 50% of all RGCs. Beta cells are responsible for processing of fine visual signals; there are two types of beta cell, on-centre and off-centre, depending on whether they respond to the onset or offset of light stimulation. This physiological distinction of on- and off-centre is reflected in the cell's anatomical structure, since their dendrites ramify in different sublayers of the inner plexiform layer (Kuffler, 1953; Famiglietti & Kolb, 1976, see also Fig. 1). During development, the dendritic trees are initially rather diffuse, before selectively refining in just one of the sublayers; furthermore, this dendritic refinement is dependent on neural activity during development (Bodnarenko & Chalupa, 1993), suggesting a role for extrinsic factors in determining the fate of a cell to become either on- or

off-centre. For example, neighbouring cells could effectively compete with each other for innervation from bipolar cells, which would then decide whether a RGC will become on- or off-centre (Kirby & Steineke, 1996). Such a competitive scheme could be seen as a version of lateral inhibition of cell fate, with on- and off-centre being the two alternative fates for a beta RGC.

An alternative mechanism suggested for the development of RGC mosaics is that each population (on- or off-centre) of cells is initially randomly arranged and then developmental cell death removes cells to sculpt out an adult-like mosaic pattern (Jeyarasasingam *et al.*, 1998). This hypothesis was based on correlating two observations: (1) alpha RGC density drops 20% postnatally and (2) regularity of alpha RGC mosaics increases from random to regular during the same postnatal period. To investigate whether either mechanisms could reliably generate the known beta RGC mosaics, we built computer models of each process to see whether the models could replicate the RIs observed experimentally for beta RGCs (Eglen & Willshaw, 2002).

7.1 *Lateral inhibition of cell fate*

The first approach was to test whether cell fate mechanisms were sufficient to transform an array of beta cells into two regular arrays of on- and off-centre cells. Specifically, what kinds of mosaics emerge if some randomly arranged undifferentiated cells inhibit each other to become either primary or secondary fate? The work from Collier *et al.* (1996) shows that for hexagonally arranged cells competing with their neighbours, the ratio of primary:secondary fate cells is 1:3. (Here we arbitrarily assume that on-centre cells are primary fate and off-centre cells are secondary fate.) However, on- and off-centre cells are thought to occur in equal numbers (1:1), rather than 1:3. Trivially, however, if the notion of neighbourhood is changed in the Collier *et al.* model, so that each cell interacts with only its nearest neighbour (perhaps due to limited signalling resources), the ratio of the number of primary to secondary fate cells is 1:1. The second change, however, to the Collier *et al.* model is to allow undifferentiated cells to be positioned randomly within the surface, rather than in a regular hexagonal grid. To test the effect of the degree of spatial order in the undifferentiated cells, we have used the $d_{\min}$ model to create the cell locations using different values of $d_{\min}$ (Eglen *et al.*, 2000).

7.1.1 *Results.*

Figure 7 shows the effects of applying the lateral inhibition model to undifferentiated cells arranged according to the $d_{\min}$ model. Lateral inhibition has divided the cells into two groups, such that the nearest neighbour of each cell is of the opposite type. If the packing intensity of the undifferentiated cells is low enough (< 0.2), the mosaic of primary and secondary fate cells is more regular than the mosaic of undifferentiated cells. However, this is no longer true if the initial mosaic is sufficiently regular (with an RI of around 4). In this case, the resulting primary and secondary fate mosaics are less regular than the initial undifferentiated population (Eglen & Willshaw, 2002). Comparison with the experimental data is deferred to section 7.3.

7.2 *Cell death*

Jeyarasasingam *et al.* (1998) observed around 20% cell death in the alpha RGC population postnatally and that on- and off-centre alpha RGC mosaics change from a random to a regular distribution during that period. Assuming that alpha and beta mosaics develop according to the same principles, we have tested whether this magnitude of cell death is sufficient to produce regular spatial distributions from initial random distributions (Eglen & Willshaw, 2002). Rather than try to model the mechanisms of cell death (which are many and varied), we took the approach of measuring the degree to which regularity

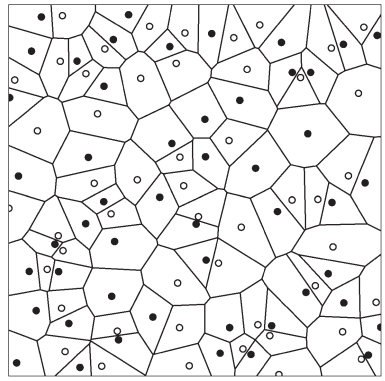

FIG. 7. Application of the lateral inhibition model (Section 6.1) to the formation of beta RGC mosaics. A total of 100 cells were positioned randomly subject to a small minimal distance constraint. Each cell then competed with its nearest neighbour through Delta–Notch signalling. At steady state, cells with high Delta levels acquired primary fate (open circles) and cells with low Delta levels acquired secondary fate (filled circles). In this example, the RI of the undifferentiated population (2.0) was lower than either that of just the primary fate cells (3.4) or that of the secondary fate cells (3.9).

would be improved by removing cells that were too close to neighbouring cells. Cells were initially randomly placed across the surface. The cell with the smallest nearest neighbour distance (or smallest Voronoi domain area) was killed; this continued until some percentage (up to 40%) of cells were removed.

7.2.1 *Results.* Figure 8 shows the results of deleting up to 40% of cells from an initial population of cells positioned at random. Before any cell death occurred, mosaic RI was around 2, indicative of a random array. Three different mechanisms were evaluated. The highest increase in RI was obtained when cells were deleted if they were too close to neighbouring cells. This intuitively makes sense as it removes small nearest neighbour distances from the overall distribution of nearest neighbours. If cells were deleted according to their size of Voronoi areas, slightly lower RIs were obtained. Finally, choosing cells at random to be deleted does not improve regularity, as expected, since this is equivalent to initially generating mosaics with lower density. These estimates of the effect of cell death upon regularity are likely to be overestimates, since the model assumes that all nearest neighbour distances are considered before the cell with the smallest nearest neighbour distance is killed. Even if the nervous system uses such a principle, it is likely to be more probabilistic, with the chances of dying increasing as the proximity to other neurons decreases.

7.3 *Evaluation of cell fate and cell death hypotheses for RGC mosaic formation*

Figure 8 shows the typical ranges of RI that the cell fate and cell death models can generate. Do these RI values approximate what is seen experimentally? There are few published mosaics of alpha and beta RGC mosaics (Wässle *et al.*, 1981a,b; Zhan & Troy, 2000), but as a rough guide, the RI of an on- or off-centre mosaic is around 5, whereas the RI of all alpha or beta cells (i.e. ignoring the cell polarity) is around 2.5. Neither cell fate nor cell death alone can replicate these experimental estimates (Fig. 9) from random starting conditions. This suggests that neither mechanism is sufficient, by itself, to replicate the experimental mosaics. However, this is not to say that these mechanisms may not be involved. If we start with one randomly arranged group of undifferentiated cells and first apply lateral inhibition, we will create two mildly regular mosaics (each with RI of around 3). If we then independently apply cell death

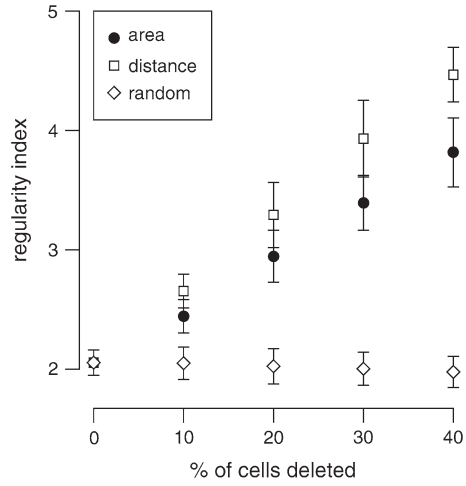

FIG. 8. Effects of cell death upon improving mosaic regularity. A total of 400 cells were initially placed randomly across the surface. Cells were iteratively deleted according to whether they had either the smallest Voronoi domain area (filled circles), smallest nearest neighbour distance (open square), or were chosen randomly (open diamond). Error bars denote ±1 s.d. of the mean, measured over 10 simulations in each condition. Data redrawn from Eglen & Willshaw (2002).

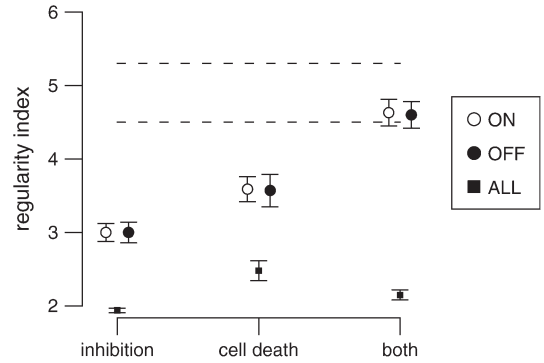

FIG. 9. Evaluation of cell fate and cell death mechanisms to account for the formation of cat beta RGC mosaics. For each mechanism, we plot the resulting RI of the on cells (open circles), the off cells (filled circles) and all cells, irrespective of polarity (filled squares). Error bars denote ±1 s.d. of the mean, with results averaged over 10 runs per condition with different initial conditions. To generate the on- and off-centre cells under the cell death hypothesis, the univariate model described in Section 7.2 was run twice, assuming that there are no interactions between on- and off-centre cells. The horizontal dotted lines represent the estimated range of RI for on- and off-centre cells from experimental maps. Neither lateral inhibition of cell fate (column 1; Section 7.1) nor cell death (column 2; Section 7.2) alone can generate on- and off-centre mosaics as regular as observed experimentally. However, combining the two methods (column 3, labelled 'both') does produce mosaics of similar regularity to those observed experimentally.

to both mosaics, the regularity of each mosaic increases to the values reported experimentally. Recent analysis of the adult bivariate RGC patterns suggests, however, that there are limited spatial interactions between positioning of on- and off-centre cells (Eglen *et al.*, 2005). Therefore, if cell fate creates any spatial dependencies in the bivariate pattern during development, cell death may subsequently mask that dependency.

8. Discussion

Phenomenological models of mosaic formation, such as the exclusion zone models, show that retinal mosaics can arise from local interactions between cells rather than requiring some global patterning system. In this review, I have considered several developmental mechanisms by which such exclusion zones could be created during development. Mathematical modelling of these developmental processes has helped us understand what types of mosaics might be created by these processes. Furthermore, by building models, we can hypothesise what might happen when such mechanisms are put together. This was demonstrated in the case of the beta RGCs, when lateral inhibition of cell fate converted an undifferentiated population into two types of cells, after which cell death then further refined the regularity of the two mosaics.

The models presented in this review are clearly starting points for future research, both in the retina and beyond. Most models to date have considered only the role of homotypic interactions upon mosaic formation, guided by the experimental observations that spatial cross-correlations are rare (Rockhill *et al.*, 2000). However, given that the different types of retinal neuron can be found within the same retinal layer, interactions between them may be possible and should be considered. Also, modelling may also investigate the functional roles of retinal mosaics. It is often assumed (as in this review) that regular mosaics are required so that the visual world is uniformly sampled. However, this may apply only to the photoreceptors; other types of retinal neuron may not need to be regularly spaced, as long as they make appropriate connections with their pre- and postsynaptic targets. Instead, having cells arranged in regular mosaics will help the process of forming appropriate connections (Galli-Resta, 2002). Hence, the effect of cellular spacing upon wiring the retina should be examined. Finally, do the principles of retinal organisation also apply to other parts of the central nervous system? To address this question, the modelling and analytical techniques will need extending to cope with positioning in 3D, which should be straightforward.

Theoretical approaches are currently limited by experimental data available. It is currently difficult to reliably label particular types of retinal neuron early enough in development, and so often only the end result of developmental processes can be observed. Models therefore are evaluated on whether they can match the observable adult-like patterns, rather than the harder, but more informative, task of replicating the same developmental changes in mosaic patterns. The increasing availability of neurochemical markers that can reliably labels cells early in development should help in this regard. Furthermore, time-lapse imaging of cell migration and rearrangement will provide much richer data sets to model rather than static observations at different developmental time points; such time-lapse imaging has already been successfully applied to understanding synaptic refinement (Kasthuri & Lichtman, 2004). Having time-lapse data of retinal neurons as they migrate and rearrange during development will allow us to build richer theories of how retinal mosaics form.

Acknowledgements

Thanks to Julian Budd for critical reading of the manuscript.

References

Ahnelt, P. K., Fernández, E., Martinez, O., Bolea, J. A. & Kübber-Heiss, A. (2000) Irregular S-cone mosaics in felid retinas. Spatial interaction with axonless horizontal cells, revealed by cross correlation. *J. Opt. Soc. Am. A*, **17**, 580–588.

BODNARENKO, S. R. & CHALUPA, L. M. (1993) Stratification of ON and OFF ganglion cell dendrites depends on glutamate-mediated afferent activity in the developing retina. *Nature*, **364**, 144–146.

CAMERON, D. A. & CARNEY, L. H. (2004) Cellular patterns in the inner retina of adult zebrafish: quantitative analyses and a computational model of their formation. *J. Comp. Neurol.*, **471**, 11–25.

CELLERINO, A., NOVELLI, E. & GALLI-RESTA, L. (2000) Retinal ganglion cells with NADPH-diaphorase activity in the chick form a regular mosaic with a strong dorsoventral asymmetry that can be modelled by a minimal spacing rule. *Eur. J. Neurosci.*, **12**, 613–620.

COLLIER, J. R., MONK, N. A. M., MAINI, P. K. & LEWIS, J. H. (1996) Pattern formation by lateral inhibition with feedback: a mathematical model of Delta-Notch intracellular signalling. *J. Theor. Biol.*, **183**, 429–446.

COOK, J. E. (1996) Spatial properties of retinal mosaics: an empirical evaluation of some existing measures. *Vis. Neurosci.*, **13**, 15–30.

COOK, J. E. (1998) Getting to grips with neuronal diversity. *Development and Organization of the Retina* (L. M. Chaulpa & B. L. Finlay eds). New York: Plenum Press, pp. 91–120.

COOK, J. E. & CHALUPA, L. M. (2000) Retinal mosaics: new insights into an old concept. *Trends Neurosci.*, **23**, 26–34.

DIGGLE, P. J. (2002) *Statistical Analysis of Spatial Point Patterns*, 2nd edn. London: Edward Arnold.

DIGGLE, P. J., EGLEN, S. J. & TROY, J. B. (2006) Modelling the bivariate spatial distribution of amacrine cells. *Case Studies in Spatial Point Process Modelling* (A. Baddeley, P. Gregori, J. Mateu, R. Stoica & D. Stoyan eds). Lecture Notes in Statistics, vol. 185. New York: Springer, pp. 215–233.

DIGGLE, P. J. & GRATTON, R. J. (1984) Monte Carlo methods of inference for implicit statistical models. *J. R. Stat. Soc. B*, **46**, 193–227.

EGLEN, S. J., DIGGLE, P. J. & TROY, J. B. (2005) Homotypic constraints dominate positioning of on- and off-centre beta retinal ganglion cells. *Vis. Neurosci.* **22**, 859–871.

EGLEN, S. J., GALLI-RESTA, L. & REESE, B. E. (2003) Theoretical models of retinal mosaic formation. *Modeling Neural Development* (A. van Ooyen ed). MIT Press, Cambridge, MA, pp. 133–150.

EGLEN, S. J., VAN OOYEN, A. & WILLSHAW, D. J. (2000) Lateral cell movement driven by dendritic interactions is sufficient to form retinal mosaics. *Netw. Comput. Neural Syst.*, **11**, 103–118.

EGLEN, S. J. & WILLSHAW, D. J. (2002) Influence of cell fate mechanisms upon retinal mosaic formation: a modelling study. *Development*, **129**, 5399–5408.

FAMIGLIETTI, JR., E. V. & KOLB, H. (1976) Structural basis for ON- and OFF-center responses in retinal ganglion cells. *Science*, **194**, 193–195.

FINLAY, B. L. & PALLAS, S. L. (1989) Control of cell number in the developing mammalian visual system. *Prog. Neurobiol.*, **32**, 207–234.

FRANKFORT, B. J. & MARDON, G. (2002) R8 development in the Drosophila eye: a paradigm for neural selection and differentiation. *Development*, **129**, 1295–1306.

GALLI-RESTA, L. (2000) Local, possibly contact-mediated signalling restricted to homotypic neurons controls the regular spacing of cells within the cholinergic arrays in the developing rodent retina. *Development*, **127**, 1509–1516.

GALLI-RESTA, L. (2002) Putting neurons in the right places: local interactions in the genesis of retinal architecture. *Trends Neurosci.*, **25**, 638–643.

GALLI-RESTA, L. & NOVELLI, E. (2000) The effects of natural cell loss on the regularity of the retinal cholinergic arrays. *J. Neurosci.*, **20**, 1–5.

GALLI-RESTA, L., NOVELLI, E., KRYGER, Z., JACOBS, G. H. & REESE, B. E. (1999) Modelling the mosaic organization of rod and cone photoreceptors with a minimal-spacing rule. *Eur. J. Neurosci.*, **11**, 1461–1469.

GALLI-RESTA, L., NOVELLI, E. & VIEGI, A. (2002) Dynamic microtubule-dependent interactions position homotypic neurones in regular monolayered arrays during retinal development. *Development*, **129**, 3803–3814.

GALLI-RESTA, L., RESTA, G., TAN, S.-S. & REESE, B. E. (1997) Mosaics of Islet-1-expressing amacrine cells assembled by short-range cellular interactions. *J. Neurosci.*, **17**, 7831–7838.

HONDA, H., TANEMURA, M. & YOSHIDA, A. (1990) Estimation of neuroblast numbers in insect neurogenesis using the lateral inhibition hypothesis of cell differentiation. *Development*, **110**, 1349–1352.

JARMAN, A. P. (2000) Developmental genetics: vertebrates and insects see eye to eye. *Curr. Biol.*, **10**, R857–R859.

JEYARASASINGAM, G., SNIDER, C. J., RATTO, G. M. & CHALUPA, L. M. (1998) Activity-regulated cell death contributes to the formation of on and off alpha ganglion cell mosaics. *J. Comp. Neurol.*, **394**, 335–343.

KASTHURI, N. & LICHTMAN, J. W. (2004) Structural dynamics of synapses in living animals. *Curr. Opin. Neurobiol.*, **14**, 105–111.

KIRBY, M. A. & STEINEKE, T. C. (1996) Morphogenesis of retinal ganglion cells: a model of dendritic, mosaic, and foveal development. *Perspect. Dev. Neurobiol.*, **3**, 177–194.

KOUYAMA, N. & MARSHAK, D. W. (1997) The topographical relationship between two neuronal mosaics in the short wavelength-sensitive system of the primate retina. *Vis. Neurosci.*, **14**, 159–167.

KUFFLER, S. W. (1953) Discharge patterns and functional organisation of mammalian retina. *J. Neurophysiol.*, **16**, 37–68.

LIVESEY, F. J. & CEPKO, C. L. (2001) Vertebrate neural cell-fate determination: lessons from the retina. *Nat. Rev. Neurosci.*, **2**, 109–118.

MEIR, E., VON DASSOW, G., MUNRO, E. & ODELL, G. M. (2002) Robustness, flexibility, and the role of lateral inhibition in the neurogenic network. *Curr. Biol.*, **12**, 778–786.

MOCHIZUKI, A. (2002). Pattern formation of cone mosaic in the zebrafish retina: a cell rearrangement model. *J. Theor. Biol.*, **215**, 345–361.

O'LEARY, D. D. M., FAWCETT, J. W. & COWAN, W. M. (1986) Topographic targeting errors in the retinocollicular projection and their elimination by ganglion cell death. *J. Neurosci.*, **6**, 3692–3705.

OWEN, M. R., SHERRATT, J. A. & WEARING, H. J. (2000) Lateral induction by juxtacrine signalling is a new mechanism for pattern formation. *Dev. Biol.*, **217**, 54–61.

PERRY, V. H. & LINDEN, R. (1982) Evidence for dendritic competition in the developing retina. *Nature*, **297**, 683–685.

RAVEN, M. A., EGLEN, S. J., OHAB, J. J. & REESE, B. E. (2003) Determinants of the exclusion zone in dopaminergic amacrine cell mosaics. *J. Comp. Neurol.*, **461**, 123–136.

RAYMOND, P. A. & BARTHEL, L. K. (2004) A moving wave patterns the cone photoreceptor mosaic array in the zebrafish retina. *Int. J. Dev. Biol.*, **48**, 935–945.

REESE, B. E., HARVEY, A. R. & TAN, S.-S. (1995) Radial and tangential dispersion patterns in the mouse retina are cell-class specific. *Proc. Natl Acad. Sci. USA*, **92**, 2494–2498.

REESE, B. E., NECESSARY, B. D., TAM, P. P. L., FAULKNER-JONES, B. & TAN, S.-S. (1999) Clonal expansion and cell dispersion in the developing mouse retina. *Eur. J. Neurosci.*, **11**, 2965–2978.

RESTA, V., NOVELLI, E., DI VIRGILIO, F. & GALLI-RESTA, L. (2005) Neuronal death induced by endogenous extracellular ATP in retinal cholinergic neuron density control. *Development*, **132**, 2873–2882.

RIPLEY, B. D. (1977) Modelling spatial patterns (with discussion). *J. R. Stat. Soc. B*, **39**, 172–212.

ROBINSON, S. R. (1991) Development of the mammalian retina. *Neuroanatomy of the Visual Pathways and Their Development* (B. Dreher & S. R. Robinson eds). Houndmills: Macmillan Press, pp. 69–128.

ROCKHILL, R. L., EULER, T. & MASLAND, R. H. (2000) Spatial order within but not between types of retinal neurons. *Proc. Natl Acad. Sci. USA*, **97**, 2303–2307.

RODIECK, R. W. (1991) The density recovery profile: a method for the analysis of points in the plane applicable to retinal studies. *Vis. Neurosci.*, **6**, 95–111.

RODIECK, R. W. (1998) *The First Steps in Seeing*. Sunderland, MA, Sinauer.

RODIECK, R. W. & MARSHAK, D. W. (1992) Spatial density and distribution of choline acetyltransferase immunoreactive cells in human, macaque and baboon retinas. *J. Comp. Neurol.*, **321**, 46–64.

RUGGIERO, C., BENVENUTI, S., BORCHI, S. & GIACOMINI, M. (2004) Mathematical model of retinal mosaic formation. *Biosystems*, **76**, 113–120.

SCHEIBE, R., SCHNITZER, J., RÖHRENBECK, J., WOHLRAB, F. & REICHENBACH, A. (1995) Development of A-type (axonless) horizontal cells in the rabbit retina. *J. Comp. Neurol.*, **354**, 438–458.

SHAPIRO, M. B., SCHEIN, S. J. & DEMONASTERIO, F. M. (1985) Regularity and structure of the spatial pattern of blue cones of macaque retina. *J. Am. Stat. Assoc.*, **80**, 803–812.

STERLING, P. (1983) Microcircuitry of the cat retina. *Annu. Rev. Neurosci.*, **6**, 149–185.

TANEMURA, M. (1979) On random complete packing by discs. *Ann. Inst. Stat. Math*, **31**, 351–365.

TANEMURA, M., HONDA, H. & YOSHIDA, A. (1991) Distribution of differentiated cells in a cell sheet under the lateral inhibition rule of differentiation. *J. Theor. Biol.*, **153**, 287–300.

TOHYA, S., MOCHIZUKI, A. & IWASA, Y. (1999) Formation of cone mosaic of zebrafish retina. *J. Theor. Biol.*, **200**, 231–244.

TOHYA, S., MOCHIZUKI, A. & IWASA, Y. (2003) Difference in the retinal cone mosaic pattern between zebrafish and medaka: cell-rearrangement model. *J. Theor. Biol.*, **221**, 289–300.

TURNER, D. L. & CEPKO, C. L. (1987) A common progenitor for neurons and glia persists in rat retina late in development. *Nature*, **328**, 131–136.

TYLER, M. J., CARNEY, L. H. & CAMERON, D. A. (2005) Control of cellular pattern formation in the vertebrate inner retina by homotypic regulation of cell-fate decisions. *J. Neurosci.*, **25**, 4565–4576.

VAN OOYEN, A. & VAN PELT, J. (1994) Activity-dependent outgrowth of neurons and overshoot phenomena in developing neural networks. *J. Theor. Biol.*, **167**, 27–43.

WAID, D. K. & MCLOON, S. C. (1998) Ganglion cells influence the fate of dividing retinal cells in culture. *Development*, **125**, 1059–1066.

WÄSSLE, H., BOYCOTT, B. B. & ILLING, R. B. (1981a) Morphology and mosaic of on-beta and off-beta cells in the cat retina and some functional considerations. *Proc. R. Soc. Lond. Ser. B*, **212**, 177–195.

WÄSSLE, H., PEICHL, L. & BOYCOTT, B. B. (1981b) Morphology and topography of on-alpha and off-alpha cells in the cat retina. *Proc. R. Soc. Lond. Ser. B*, **212**, 157–175.

WÄSSLE, H. & RIEMANN, H. J. (1978) The mosaic of nerve cells in the mammalian retina. *Proc. R. Soc. Lond. Ser. B*, **200**, 441–461.

WEBB, S. D. & OWEN, M. R. (2004) Oscillations and patterns in spatially discrete models for developmental ligand-receptor interactions. *J. Math. Biol.*, **48**, 444–476.

ZHAN, X. J. & TROY, J. B. (2000) Modeling cat retinal beta-cell arrays. *Vis. Neurosci.*, **17**, 23–39.